Pretel-Jolis, R.; Robles Martínez, Á.; Ruano García, MV.; Seco, A.; Ferrer, J. (2016). A plant-wide energy model for wastewater treatment plants: application to anaerobic membrane bioreactor technology. Environmental Technology. 37(18):2298-2315. https://doi.org/10.1080/09593330.2016.1148903

A plant-wide energy model for WWTPs: application to AnMBR technology

R. Pretel[a,*], A. Robles[a], M.V. Ruano[b], A. Seco[b] and J. Ferrer[a]

[a] Institut Universitari d'Investigació d'Enginyeria de l'Aigua i Medi Ambient, IIAMA, Universitat Politècnica de València, Camí de Vera s/n, 46022 Valencia, Spain (e-mail: *rutprejo@upv.es; ngerobma@upv.es; jferrer@hma.upv.es*)

[b] Departament d'Enginyeria Química, Escola Tècnica Superior d'Enginyeria, Universitat de València, Avinguda de la Universitat s/n, 46100 Burjassot, Valencia, Spain (e-mail: *m.victoria.ruano@uv.es; aurora.seco@uv.es)*

* Corresponding author: tel. +34 96 387 61 76, fax +34 96 387 90 09, e-mail: *rutprejo@upv.es*

Abstract

The aim of this study is to propose a detailed and comprehensive plant-wide model for assessing the energy demand of different wastewater treatment systems (beyond the traditional activated sludge) at both steady- and unsteady-state conditions. The proposed model enables calculating power and heat energy requirements (*W* and *Q*, respectively), and energy recovery (power and heat) from methane and hydrogen capture. In order to account for the effect of biological processes on heat energy requirements, the model has been coupled to the extended version of the plant-wide mathematical model BNRM2, which is implemented in the simulation software DESASS. Two case studies have been evaluated to assess the model performance: (1) modelling the energy demand of two urban WWTPs based on conventional activated sludge (CAS) and submerged anaerobic MBR (AnMBR) technologies at steady-state conditions; and (2) modelling the dynamics in reactor temperature and heat energy requirements in an AnMBR plant at unsteady-state conditions. The results indicated that the proposed model can be used for assessing the energy performance of different wastewater treatment processes, thus being useful for different purposes, e.g. WWTP design or upgrading, or development of new control strategies for energy savings.

Keywords

Anaerobic MBR; BNRM2; DESASS; plant-wide energy model; wastewater treatment.

1. Introduction

Wastewater treatment is an energy-intensive activity whose energy costs vary considerably from one wastewater treatment plant (WWTP) to another, depending on the type of influent, treatment technology and required effluent quality. Different environmental concerns (e.g. global warming and greenhouse gases (GHG) emissions) are some of the driving factors promoting changes in the wastewater treatment field [1]. Indeed, sustainable water management is increasingly important for utilities and is driving efforts to reduce energy consumption in WWTPs without compromising effluent quality. Specially, energy saving is the fastest, highest impacting and most cost-effective way of reducing GHG emissions [2]. Therefore, energy saving in WWTPs is a key point for improving overall environmental performance in wastewater treatment domain [3].

Besides actions focussed on saving energy and increase energy efficiency, the expansion of renewable energies is viewed to be an important factor for a secure energy future [4]. In this respect, since the water-energy-carbon nexus is gaining increasing importance as a field of research, biogas production from sewage sludge digestion is a subject of interest in both energy and wastewater domains [5]. Part of the energy recovered from wastewater in the form of biogas is usually used for heating purposes, whilst the rest can be employed for meeting WWTP power requirements after conversion to electrical power. Hence, the possibility of energy recovery from wastewater is a key operating opportunity in the wastewater treatment field in order to find energy savings thus reducing operating costs. Furthermore, biogas offers greater energy and environmental benefits when generating power and heat simultaneously using CHP (combined heat and power) technology than when generating both separately [6].

To date, the interest of the scientific community involved in the wastewater treatment field has been mainly focused on water quality and associated plant-wide modelling issues [7]. In this respect, the use of mathematical models for WWTP design and upgrading, process optimisation, operator

training, and development of control strategies has become a standard engineering tool in the last decade (see, for instance, [8, 9]. Indeed, model-based analysis seems to be a promising method for improving energy efficiency in wastewater treatment [10]. Process variables can be both tuned and optimised, and technologies can be compared in a rigorous way, especially by including energy aspects in the computations [7]. Hence, plant-wide energy models are expected to be a promising tool for selection of the best among the alternatives aimed to meet the desired criteria in the WWTP network (e.g. low energy consumption) [10].

Different studies can be found in literature dealing with energy modelling in wastewater treatment. Jeppsson et al. [11] proposed an extension of the Benchmark Simulation Model no 1 (BSM1) aimed at facilitating control strategy development and process performance evaluation at a plant-wide level, including therefore a complete energy balance. Gómez et al. [12] presented a new biochemical model for aerobic digestion that introduced an energy balance to dynamically predict the temporary evolution of temperature in an autothermal thermophilic aerobic digester. Righi et al. [13] assessed the environmental profile and energy balance of different waste treatment systems. Another representative study was conducted by Lemos et al. [14], who assessed the environmental performance and the electricity consumption of an entire urban water system; whilst Nowak et al. [15] considered several ways of ensuring positive energy balance in wastewater treatment. However, scarce literature has been found dealing with the development of a plant-wide energy model including new technologies for treating urban wastewater at full-scale, such as membrane-based ones.

On the other hand, some software in the field of wastewater engineering already included not only the analysis of process water management and sludge treatment, but also the assessment of energy consumption and efficiency (e.g gPROMS, Simba 6, W2E, WWTP/check, etc.). For instance, Tous

et al. [16] applied the simulation program W2E for calculating the energy and mass balance of different sewage sludge treatments; Descoins et al. [7] developed a plant-wide model, implemented in the modelling software gPROMS, including not only the main biochemical transformations but also the energy consumption for each involved physical unit operation; and Pijájová and Derco [17] assessed the performance of urban wastewater treatment systems using the simulator SIMBA 6. However, these modelling softwares do not include new promising technologies aimed at enhancing wastewater treatment, such as anaerobic membrane bioreactor (AnMBR).

Contrary to aerobic processes for UWW treatment, where significant energy input is required for aeration and energy recovery from organic matter is not maximised [18], AnMBR technology reduces sludge production, eliminates aeration and generates methane [19]. Hence, although AnMBR technology has not been applied to full-scale UWW treatment yet, recent literature ([20]) has reported increasing interest by the scientific community on its applicability.

Hence, the aim of this study is to propose a detailed and comprehensive plant-wide model for assessing the energy demand of different wastewater treatment systems (beyond CAS) at both steady- and unsteady-state conditions. The proposed model has been coupled to the extended version of the plant-wide mathematical model BNRM2 [21] proposed by Durán [22], which is implemented in the new version of the simulation software DESASS [9]. DESASS allows the design, upgrading, simulation and optimisation of municipal and industrial WWTPs, including, among others, aerobic membrane bioreactor (AeMBR) and AnMBR technologies. In this respect, the proposed energy model allows calculating the overall energy demand of different WWTPs, enabling therefore their analysis and improvement from an environmental point of view (e.g. reduction of GHG emissions associated with energy consumption). Specifically, the model enables calculating power and heat energy requirements (W and Q, respectively), and energy recovery

(power and heat) from methane and hydrogen capture during the anaerobic treatment of organic matter. The *W* term (power energy) entails the main equipment employed in WWTPs (e.g. blowers, pumps, diffusers, stirrers, dewatering systems, etc.). The *Q* term (heat energy) considers heat transfer through pipe and reactor walls, heat transfer due to gas decompression, external heat required when temperature is controlled, and enthalpy of the biological reactions included in the extended version of the plant-wide model BNRM2.

2. Materials and methods

2.1 Energy model description

The proposed model, which is coupled to the extended version of the plant-wide mathematical model BNRM2 [21,22], consists of a set of energy equations that could be solved for both steady and dynamic conditions. The model represents the total energy demand of the evaluated treatment scheme using Equation 1. This equation symbolises the sum of potential energy (E_p), kinetic energy (E_k), and internal (molecular) forms of energy (h) such as electrical and chemical energy, being equal to the heat transferred to the system (Q) and the work applied by the system on its surroundings (W) during a given time interval.

$$\Delta E_p + \Delta E_k + \Delta h = W + Q \qquad \text{Equation 1}$$

2.1.1. Power energy (W)

The equipment considered for calculating the *W* term (power energy) consists of the following: pumping equipment (pumps and blowers), diffusers, stirrers, circular suction scraper bridges (for primary and secondary settlers and sludge thickeners), rotofilters and sludge dewatering systems.

Table 1 shows the equations employed for calculating *W*. The energy consumption of blowers (Equation 2 and 3), general pumps (feeding and recycling) (Equation 4) and permeate pumps

(Equation 5) is calculated as proposed by Judd and Judd [23]. To calculate the net power energy required by the permeate pump ($P_{permeate}$), the sum of the power energy consumed in the following four membrane operating stages was considered: filtration ($P_{filtration}$), back-flushing ($P_{back\text{-}flushing}$), degasification ($P_{degasification}$) and ventilation ($P_{ventilation}$). Equation 5 is used to calculate the power energy consumed in filtration, back-flushing and degasification stages, whilst Equation 4 is used to calculate the power energy consumed in ventilation stage since the fluid does not pass through the membrane ([24]).

Power energy for stirring and dewatering systems is calculated by Equations 6 and 7, respectively. The default values included in DESASS for the specific energy consumption ($E_{dewatering}$) of the different types of dewatering systems considered in the model are 5-20, 15-40, 30-60 and 50-150 $kWh \cdot tSS^{-1}$ for band filter, press filter, centrifuge and vacuum filter, respectively.

2.1.2. Heat energy (Q)

Table 2 shows the equations employed for calculating *Q*. *Q* was assumed to be the sum of the following terms: external heat energy (input or output) required when temperature is controlled ($Q_{EXTERNAL,}$ Equation 8); heat energy dissipated through pipes and reactor walls ($Q_{DISSIPATED,}$ Equation 9); heat energy released or absorbed by the gas decompression process ($Q_{DECOMPRESSION,}$ Equation 13); and heat energy released or absorbed by the biological reactions taking place in the treatment unit ($Q_{ENTHALPY,}$ Equation 20). Figure 1 illustrates an example of the process flow diagram related to temperature and heat energy requirements in a closed-air reactor.

For calculating the heat energy dissipated (or gain) through the walls of the reactor ($Q_{DISSIPATED}$), the heat transfer coefficient in both surface and buried section of the reactor (see Equation 10 and 11, respectively) and the soil conductivity (see Equation 12) are taken into account. As Equation 12

shows, the relationship between soil conductivity and moisture is obtained by linear interpolation, assuming that moist soil is completely saturated on water (100 % humidity and Ks of 3.7 kcal· m^{-1}·h^{-1}·°C^{-1}) and dry soil is completely dried (0% humidity and Ks of 1.2 kcal· m^{-1}·h^{-1}·°C^{-1}).

As Figure 1 illustrates, temperature variations occurring through the gas recirculation system have been also estimated in order to calculate the heat absorbed or released in the reactor during the gas decompression process ($Q_{DESCOMPRESSION}$). To this aim, it has been assumed that the gas presents a temperature T_1 in the inlet of the recirculation system equal to the temperature of the mixed liquor inside the reactor. Then, the gas moves through the pipe from the reactor to the blower inlet causing heat loss or gain until reaching a temperature T_2 (Equation 14). In the blower the temperature is increased from T_2 to T_3 due to the gas compression process (Equation 15). Finally, the gas moves through the pipe from the blower output to the reactor causing heat loss or gain until reaching a temperature T_4 (Equation 14).

As the proposed energy model was coupled to the plant-wide model BNRM2, the enthalpy of some key biological reactions involved in wastewater treatment can be calculated. Specifically, from a total of 67 equations from the model BNRM2, 27 equations were employed for calculating molar enthalpy at a given temperature by means of Kirchhoff equation (see Equation 16). Hydrolysis, fermentation, precipitation, re-dissolution, bacterial lysis and gas stripping (see [21,22]) were not included in the model since the heat absorbed or released in these reactions was considered negligible. The empiric formulas used to determine the specific heat of solids and liquids, gases and dissolved methane are shown in Equation 17, 18 and 19, respectively (see Table 2). The standard molar enthalpy of formation at 298K and the coefficients of the molar heat capacity at constant pressure (A, B, C, D and E) for each substance are shown in Table S1 (Supplementary Data). Table 3 shows the biological reactions (including its corresponding molar enthalpy) considered in the

proposed energy model. To convert the molar enthalpy of the reactions (kcal·mol^{-1}) to heat units ($Q_{ENTHALPY}$, kcal·h^{-1}), the stoichiometric matrix and kinetics of the biological reactions included in the BNRM2 are used (see Equation 20 in Table 2).

2.1.3. Energy recovery from methane capture

CHP technology is used as alternative to conventional energy generation systems. CHP consists of cogeneration through which electrical and heat energy production occurs simultaneously, obtaining an overall efficiency of up to 70-80%. In WWTPs, CHP technology transforms the hydrogen and methane obtained during the anaerobic digestion of organic matter into heat and power energy, considering the efficiency of the different CHP technologies according to EPA [25].

Table 4 shows the equations employed in the model for calculating the energy recovery from methane and hydrogen capture in terms of heat ($Q_{methane,}$ Equation 21) and power ($W_{methane}$, Equation 22). The maximum allowable concentration of H_2S (see Equation 23 in Table 4) in the biogas entering CHP motors (e.g microturbine for cogeneration) was set to 70 mg·MJ^{-1} biogas [26].

2.2 Implementation of the energy model in the simulation software DESASS

Ferrer et al. [9] developed a computational software called DESASS for designing, simulating and optimising both aerobic and anaerobic wastewater treatment technologies, considering the most important physical, chemical and biological processes taking place in a traditional WWTP. Afterwards, DESASS was extended and updated for including new technologies such as SHARON, BABE, AeMBR and AnMBR. Moreover, DESASS incorporates a tool for designing the whole aeration system (i.e. blowers, piping and valve system, diffusers and their supports). As commented before, the simulation software incorporates an extended version of the plant-wide model BNRM2 [21], including the competition between both acetogenic and methanogenic microorganisms and sulphate-reducing microorganisms [22]. This mathematical model was validated beforehand using

experimental data obtained from different wastewater treatment processes (see, for instance, [27,28,29,30]), including AnMBR likewise [22]. Apart from being useful for designing, simulating and optimising WWTPs in terms of process performance, DESASS has been updated for incorporating an energy model toolbox entailing the proposed plant-wide energy model. The principles guiding the development of this toolbox are user friendliness and flexibility to incorporate several elements involving power and heat energy demand in different WWTPs.

Figure S1 (Supplementary Data) shows some of the windows that can be generated in DESASS by using the developed toolbox. In particular, this figure shows the design parameters related to the power energy requirements of a blower (Figure S1a); and the heat energy requirements in an AnMBR (Figure S1b). In order to calculate the energy demand of a WWTP through the proposed tool, the following steps must be trailed:

(1) Creating a wastewater treatment layout incorporating both treatment units (e.g. settler, reactor, digester, thickener, dewatering system, etc…) and mechanical elements (e.g. pumps, blowers, diffusers, rotofilter, mechanical stirrers, circular suction scraper bridges, and sludge dewatering system).

(2) Defining all the necessary design parameters related to power and heat energy requirements (see Figure S1).

(3) Simulating the defined layout in order to obtain the results from the applied model.

Once the simulations have been finished, DESASS provides the energy model results of the evaluated system, including the before-mentioned terms: power requirements, heat energy requirements, cogenerated energy, and net energy demand. Moreover, the power energy requirements of each mechanical element and the heat energy requirements of each treatment unit can be shown independently clicking on the elements included in the designed layout.

Design parameters related to power energy requirements

Regarding the design of pumps and liquid pipelines, the toolbox allows the user editing the following terms: height difference in fluid level between two treatment units connected by a pumping system; engine and pump efficiency; and inlet and outlet pipe characteristics. As regards pipe characteristics, the following terms can be edited: material in order to establish the roughness and conductivity; either nominal diameter and fluid velocity for calculating the number of pipes or number of pipes and fluid velocity for calculating the nominal diameter; thickness; length; and equivalent length of accessories.

Regarding the design of blowers and gas pipelines, the toolbox allows the user editing the following terms: headspace pressure in closed-air reactors; type of compression (adiabatic and isentropic, isothermal or polytropic); branch and model of the diffusers in order to calculate the head loss; inlet and outlet pipe characteristics (same terms as liquid pipelines); and engine and blower efficiency.

In order to calculate the real power energy requirements of pumps and blowers, the toolbox allows selecting commercial equipment extracted from an editable database including the following specifications: model, branch, flow, pressure and motor power. Flow, pressure and theoretical power consumption are calculated using Equations 2 to 5, and are compared to those included in the database in order to propose a list of equipment fitting the requirements of the evaluated layout.

Regarding the design of stirrers, the user is able to edit power energy consumption in terms of $W \cdot m^{-3}$ and efficiency. Therefore, the toolbox compares the theoretical power requirements of the stirrer (calculated using the corresponding tank volume) to the power requirements from commercial equipment included in the editable database in order to propose a list of equipment fitting the design

specifications. Concerning the dewatering system, the user is able to edit type (e.g. band filter, press filter, centrifuge and vacuum filter) and efficiency, thus the toolbox automatically selects power energy consumption in terms of $kWh \cdot tSS^{-1}$ in order to calculate the power requirements of the selected item. As regards rotofilter, the user is able to edit the motor power in terms of W; whilst for circular suction scraper bridges, the toolbox provides a list of models from the database that fit the corresponding motor power by selecting the unit branch.

Hence, the toolbox includes a database for selecting commercial equipment fitting the design criteria. This database can be edited by the user in order to incorporate new equipment.

Design parameters related to heat energy requirements

In order to calculate the heat energy dissipated through the walls of the reactor, the toolbox allows the user editing the temperature inside and outside the reactor, the temperature of the inflow, the type and thickness of reactor material (in order to calculate the conductivity), the type and thickness of insulating material (in order to calculate the conductivity), the reactor geometry and dimensions, the % of the outer reactor, the % of soil humidity and the thickness of the soil in contact with the reactor.

As previously mentioned, the toolbox allows the user editing the design parameters of the blower (e.g. headspace reactor pressure, type of compression, inlet and outlet pipe characteristics, etc.) in order to calculate the heat energy released or absorbed by the gas decompression process.

Moreover, the user is able to choice one of the two following options for heat energy calculation: (1) operating at fixed temperature thus simulating total heat energy requirements; or (2) operating at fixed heat energy requirements thus simulating system temperature.

Design parameters of cogeneration energy

For the cogeneration system, it is possible to select the type of CHP system to be used (e.g. steam turbine, reciprocating internal combustion engine, gas/combustion turbine and microturbine) in order to calculate power and heat energy production efficiency and also the efficiency of the heat exchanger. Therefore, the tool calculates the power and heat energy recovery from hydrogen and methane capture (biogas and dissolved methane in the effluent).

3. Case study

3.1 Modelling energy demand in a CAS and AnMBR urban WWTP at steady-state conditions

3.1.1 Design and operating parameters

The performance of the proposed plant-wide energy model at steady-state conditions is illustrated in this study by two case-specific examples of urban WWTP, including as main treatment technology: 1) CAS, and 2) AnMBR coupled to an aerobic-based post-treatment for nutrient removal. These treatment schemes were designed for meeting the European discharge quality standards (sensitive areas and population of more than 100000 p-e) as regards solids (<35 $mg \cdot L^{-1}$ of tSS), organic matter (<125 and 25 $mg \cdot L^{-1}$ of COD and BOD, respectively) and nutrients (<10 and 1 $mg \cdot L^{-1}$ of N and P, respectively). It is worth to point out that chemical removal of phosphorus was assumed in both cases for meeting phosphorous effluent standards. In addition, a maximum value of 35% of biodegradable volatile suspended solids (BVSS) was considered as sludge stabilisation criteria.

The AO (anoxic – oxic) configuration was selected for designing the aerobic-based treatment units (CAS-based WWTP and post-treatment unit in the AnMBR-based WWTP). It is important to note that CAS was represented in this study as an anoxic-oxic process rather than an aerobic activated sludge process.The volume of anoxic and oxic tanks was 40 and 60% of total reactor volume, respectively.

Figure 2 shows the main window of DESASS with the layout of the CAS- and AnMBR-based WWTPs evaluated in this study. These treatment schemes were designed and simulated for a treatment flow rate of 50000 $m^3 \cdot day^{-1}$ and ambient temperature of 20 ºC. The full characterisation of the urban wastewater (UWW) used in this study is shown in Table 5. This characterisation corresponds with the effluent from the pre-treatment of the Carraixet WWTP (Valencia, Spain). Two simulation scenarios were evaluated: the treatment of sulphate-rich UWW (9.45 mg $COD \cdot mg^{-1}$ SO_4-S, corresponding with an influent sulphate concentration of 100 mg SO_4-$S \cdot L^{-1}$); and the treatment of low-sulphate UWW (94.5 mg $COD \cdot mg^{-1}$ SO_4-S, corresponding with an influent sulphate concentration of 10 mg SO_4-$S \cdot L^{-1}$). Methane capture efficiency was set to 100% in this case study.

CAS technology: As commented before, the CAS unit consisted of an AO (anoxic – oxic) configuration, which was operated at hydraulic retention time (HRT) of 24 hours, sludge retention time (SRT) of 10 days and mixed liquor suspended solids (MLSS) concentration of 2.3 $g \cdot L^{-1}$. An anaerobic digester (operating at 35 ºC) was also included as main element of the CAS-based WWTP to meet the sludge stabilisation criteria. Heat energy input was needed to maintain a temperature of 35 ºC in the anaerobic digester unit. Biogas was considered to be captured from the anaerobic digester unit and used to generate energy.

AnMBR technology: The AnMBR unit was operated at HRT of 18 hours, SRT of 40 days, 20 ºC-standardised transmembrane flux (J_{20}) of 20 LMH, specific gas demand per square metre of membrane area (SGD_m) of 0.1 $m^3 \cdot m^{-2} \cdot h^{-1}$ and MLSS in the membrane tank of 14 $g \cdot L^{-1}$. This operating mode resulted in minimum filtration costs in previous studies [31,32]. Further digestion of the sludge was not required since the AnMBR unit was already designed for meeting the sludge

stabilisation criteria. Biogas and methane dissolved in the effluent were both considered to be captured and used to generate energy.

A post-treatment step based on AO (anoxic – oxic) configuration with chemical addition for phosphorous removal was included in the AnMBR-based treatment scheme in order to meet nutrient effluent standards. This step contemplated two possibilities: AeMBR- and CAS-based post-treatment. The AeMBR-based post-treatment was operated at SRT of 10 days, J_{20} of 29 LMH, specific air demand per square metre of membrane area (SAD_m) of 0.3 $m^3 \cdot m^{-2} \cdot h^{-1}$ and MLSS in the membrane tank of 2.6 $g \cdot L^{-1}$; whilst the CAS-based post-treatment was operated at SRT of 10 days and MLSS concentration of 2.3 $g \cdot L^{-1}$. A fraction of the influent wastewater was bypassed anyhow to the post-treatment unit in order to meet effluent quality standards (further organic matter was required for denitrification rather than the contained in the effluent from the AnMBR unit). Specifically, around 27% of the wastewater entering the AnMBR-based WWTP was derived directly to the post-treatment unit (see Figure 2).

3.1.2 Simulation results

Figure 3 shows the weighted average distribution of the simulated energy input and output for the CAS- and AnMBR-based WWTPs. As Figure 3 shows, the main term contributing the energy demand of the CAS-based WWTP was the power energy input (about 62.3%). In absolute terms, power requirements resulted in 0.48 $kWh \cdot m^{-3}$, heat energy requirements (to maintain a temperature of 35 ºC in the anaerobic digester) resulted in 245 $kcal \cdot m^{-3}$ and power and heat energy recovery from the produced biogas was 0.30 $kWh \cdot m^{-3}$ and 222 $kcal \cdot m^{-3}$, respectively. As regards the simulated AnMBR-based WWTP, energy demand was completely related to power energy input, since heat energy requirements were null due to operating at ambient temperature conditions. In absolute terms, power requirements resulted in 0.66 and 0.48 $kWh \cdot m^{-3}$ in AeMBR- and CAS-based post-treatment configurations, respectively. Power recovery from methane in both AeMBR- and CAS-based post-

treatment configurations was 0.27 and 0.45 kWh·m^{-3} when treating sulphate-rich (100 mg SO_4-S·L^{-1}) and low-sulphate (10 mg SO_4-S·L^{-1}) urban wastewater, respectively. Therefore, the energy demand of CAS technology resulted in approx. 0.21 kWh·m^{-3} whilst for AnMBR coupled to an AeMBR- and CAS-based post-treatment resulted in approx. 0.38 and 0.21 kWh·m^{-3}, respectively, when treating sulphate-rich UWW. Nevertheless, this energy demand could be reduced to 0.21 and 0.04 kWh·m^{-3} in AnMBR coupled to an AeMBR- and CAS-based post-treatment, respectively, when treating low-sulphate UWW. Hence, it can be concluded that from an energy perspective, AnMBR coupled to a CAS-based post-treatment may be a sustainable approach for UWW treatment in comparison with other existing technologies under the operating conditions and WW characteristics evaluated in this case study.

3.2 Modelling temperature and heat energy requirements in an AnMBR system at unsteady-state conditions.

3.2.1 Design and operating parameters

The performance of the proposed plant-wide energy model at unsteady-state conditions was assessed using experimental data obtained from an AnMBR plant that treated effluent from the pre-treatment of a full-scale WWTP (Valencia, Spain) (see Table 5).

The AnMBR plant consists of an anaerobic reactor with a total volume of 1.3 m^3 (0.4 m^3 head-space volume) connected to two membrane tanks each one with a total volume of 0.8 m^3 (0.2 m^3 head-space volume). Each membrane tank includes one ultrafiltration hollow-fibre membrane commercial system (PURON®, Koch Membrane Systems, 0.05 µm pore size, 30 m^2 total filtering area). A rotofilter of 0.5 mm screen size has been installed as pre-treatment system. One equalisation tank (0.3 m^3) and one CIP tank (0.2 m^3) are also included as main elements of the pilot plant. In order to control the temperature when necessary, the anaerobic reactor is jacketed and

connected to a water heating/cooling system. Further details on this AnMBR can be found in Giménez et al. [19] and Robles et al. [33].

Numerous on-line sensors and items of automatic equipment were installed in order to automate and control plant operations and provide on-line information about the state of the process [33]. The on-line sensors employed in this study consist of the following: two pH-temperature transmitters used to measure the temperature in both inflow and AnMBR; one flow indicator transmitter used for calculating the amount of mixed liquor to be heat; and one automatic valve that allows to pass water through the reactor jacket for controlling the temperature in the system. Besides the on-line process monitoring, grab samples of anaerobic sludge were taken for measuring sludge density.

As commented above, the temperature of the wastewater entering the AnMBR plant and the temperature inside the reactor were continuously recorded. Ambient temperature was obtained from a weather station located near the position of the plant. Hourly and daily average ambient temperature data was facilitated by the Spanish State Meteorological Agency [34].

According to the structure of the AnMBR plant, the following heat energy design parameters were considered for simulating the heat energy dissipated though the reactor walls: steel as reactor material, 3-cm reactor wall thickness, fiberglass as insulating material, 2-cm fiberglass thickness, cylinder and rectangular geometry for reactor and membrane tanks, respectively, 0.7-m diameter and 2.1-m height for reactor dimensions, 3-m height, 1.1-m width and 0.3-m depth for membrane tank dimensions, and 100% of outer volume.

The performance of the energy model was assessed for both short-term and long-term operation. The short-term assessment comprised an operating period of 24 hours, whilst the long-term

assessment comprised an operating period of 30 days. Both assessments aimed at evaluating the capability of the model to reproduce energy variations in AnMBRs even when operating under dynamic conditions (i.e. ambient temperature and/or inflow temperature suffered different variations).

3.2.2 Simulation results

Figure 4 illustrates the variations in both experimental and simulated reactor temperature during a 24-hour operating period (Figure 4a and Figure 4b) and during a 30-day operating period (Figure 4c). External heat energy requirements were null ($Q_{EXTERNAL}$=0, Equation 8) since the temperature in the system was not controlled (reactor free temperature). As Figure 4 shows, the reactor temperature variations were mainly related to variations in the inflow temperature and ambient temperature, affecting therefore $Q_{DISSIPATED}$ (Equation 9); $Q_{DECOMPRESSION}$ (Equation 13) and $Q_{ENTHALPY}$ (Equation 20). Overall, the proposed model was able to correctly reproduce temperature dynamics in the evaluated AnMBR system.

Figure 5 shows the simulated heat energy requirements in the AnMBR plant during a 24-hour period (Figure 5a and Figure 5b) and during a 30-day operating period (Figure 5c). All cases were run at controlled temperature of around 20ºC. Inflow and ambient temperature, as well as the time interval during which the heating or cooling valve opened, were used to evaluate the dynamics in the simulated heat energy requirements.

For the 24-hour period operating with heating system (see Figure 5a), the time interval (minutes/hour) during which the heating valve remained open varied according to variations in heat energy requirements for temperature control (see hours from 0 to 12 and from 12 to 24, respectively). Indeed, ambient temperature increased throughout the first 12 hours of operation and

decreased during the last 12 hours, affecting therefore heat energy requirements. This behaviour is in agreement with the dynamics in the simulated heat energy, which indicates that the proposed model might be capable to predict variations in heat energy requirements in the evaluated AnMBR system.

For the 24-hour period operating with cooling system (see Figure 5b), the cooling valve remained continuously opened from hours 8 to 18 (cooling time up to 60 minutes/hour). During this period, the ambient temperature increased (see hours from 8 to 14). Hence, higher external output of heat energy was required for controlling the temperature around the established set-point. Under these operating conditions, the model predicted the expected variation in heat energy requirements for controlling the reactor temperature.

As regards the long-term assesment, Figure 5c illustrates a decrease in the heating time (hours/day) during the 30-day period operating with heating system. Specifically, the time during which the heating valve remained open decreased during the first 18 days of operation due to an increase recorded in ambient temperature. From days 18 to 23 both ambient and inflow temperature decreased, resulting therefore in increased heating time. From days 23 to 28, the time interval during which the heating valve open decreased due to a new increase recorded in inflow and ambient temperature (see days from 23 to 28). As Figure 5 shows, the simulated heat energy requirements follow a similar pattern to the one expected under these operating conditions (e.g. heat energy requirements increased when ambient and inflow temperature decreased, and viceversa).

3.3 The possible role of the proposed tool in the achievement of the carbon neutral WWTP

As previously commented, plant-wide modelling in the wastewater treatment field is attractive to many researchers as it provides a holistic view of the process and it allows for a more comprehensive understanding of the interactions between unit processes. Therefore, the proposed

plant-wide energy modelling tool could represent a useful application for evaluating the energy consumption and efficiency of different wastewater treatment alternatives, focussing furthermore in reducing the associated potential environmental impact (e.g. GHG emissions). Different layouts can be easily evaluated under different influent, environmental and operating conditions, allowing to assess sustainability in the WWT field.

Therefore, this tool might be useful for supporting complex decisions for a particular problem under reduced time frames. Specifically, the tool could be helpful on determining for each specific case (i.e. implementation, upgrading and operation) whether one technology is the best available option or not. The tool could be therefore useful to justify multi-criteria decisions and provide end-users a tool to explore “what-if” scenarios.

Hence, the proposed plant-wide energy model can be used for different purposes such as WWTP design or upgrading, and development of new control strategies for energy savings and thus contributing to the pursuit of carbon neutral wastewater treatment.

5. Conclusions

This paper presents a detailed and comprehensive plant-wide model for assessing the energy demand of different wastewater treatment systems at both steady- and unsteady-state conditions. The model was able to reproduce energy variations in AnMBRs even when operating under dynamic conditions (i.e. ambient temperature and/or inflow temperature suffered different variations). The proposed plant-wide energy model could be useful for different purposes such as WWTP design or upgrading, and development of new control strategies for energy savings.

Acknowledgements

This research work has been supported by the Spanish Ministry of Science and Innovation (MICINN, Project CTM2011-28595-C02-01/02) jointly with the European Regional Development Fund (ERDF) which are gratefully acknowledged. Ambient temperature data was facilitated by the Spanish State Meteorological Agency (AEMET), which is gratefully acknowledged.

References

[1] G. Olsson, B. Carlsson, J. Comas, J. Copp, K.V. Gernaey, P. Ingildsen, U. Jeppsson, C. Kim, L. Rieger, I, Rodríguez-Roda, J.P.Steyer, I. Takács, P.A. Vanrolleghem, A. Vargas Casillas, A. Yuan, L. Åmand, Instrumentation, Control and Automation in Wastewater- from London 1973 to Narbonne 2013. Water Sci. Technol. 69 (2014), 1373-85.

[2] B. Nicolae, B. George-Vlad, Life cycle analysis in refurbishment of the buildings as intervention practices in energy saving. Energ. Buildings 86 (2015), 74–85.

[3] L. Corominas, J. Foley, J.S. Guest, A. Hospido, H.F. Larsen, S. Morera, A. Shaw, Life cycle assessment applied to wastewater treatment: State of the art. Water Res. 47 (2013), 5480-5495.

[4] A. Bauer, P. Böschb, A. Friedl, T. Amona, Analysis of methane potentials of steam-exploded wheat straw and estimation of energy yields of combined ethanol and methane production. J. Biotechnol. 142 (2009), 50-55.

[5] G. Venkatesh, R.A. Elmi, Economic-environmental analysis of handling biogas from sewage sludge digesters in WWTPs (wastewater treatment plants) for energy recovery: Case study of Bekkelaget WWTP in Oslo (Norway). Energy 58 (2013), 220-235.

[6] EPA. Environmental Protection Agency, 2015. Combined Heat and Power Partnership. Agency of the United States federal government.

[7] N. Descoins, S. Deleris, R. Lestienne, E. Trouvé, F. Maréchal, Energy efficiency in waste water treatments plants: Optimization of activated sludge process coupled with anaerobic digestion. Energy (2011) 1-12.

[8] K.V. Gernaey, M.C.M van Loosdrecht, M. Henze, M. Lind, S.B Jørgensen, Activated sludge wastewater treatment plant modelling and simulation: state of the art. Environ. Modell. Softw. 19 (2004), 763-783.

[9] J. Ferrer, A. Seco, J. Serralta, J. Ribes, J. Manga, E. Asensi, J.J. Morenilla, F. Llavador, DESASS: a software tool for designing, simulating and optimising WWTPs, Environ. Modell. Softw. 23(2008), 19-26.

[10] H. Bozkurt, A. Quaglia, K.V. Gernaey, G. Sin., G, A mathematical programming framework for early stage design of wastewater treatment plants. Environ. Modell. Softw. 64 (2015), 164-176.

[11] U. Jeppsson, C. Rosen, J. Alex, J. Copp, K.V. Gernaey, M.-N. Pons, P.A. Vanrolleghem, Towards a benchmark simulation model for plant-wide control strategy performance evaluation of WWTPs. Water Sci. Technol. 53 (2006), 287–295.

[12] J. Gómez, M. de Gracia, E. Ayesa, J.L. Garcia-Heras, Mathematical modelling of autothermal thermophilic aerobic digesters. Water Res. 41 (2007), 959-968.

[13] S. Righi, L. Oliviero, M. Pedrini, A. Buscaroli, C.D. Casa, Life Cycle Assessment of management systems for sewage sludge and food waste: centralized and decentralized approaches. J. Clean. Prod. 44 (2013), 8-17.

[14] D. Lemos, D.C. Dias, X. Gabarrell, L. Arroja, Environmental assessment of an urban water system. J. Clean. Prod. 54 (2013), 157-165.

[15] O. Nowak, P. Enderle, P. Varbanov, Ways to optimize the energy balance of municipal wastewater systems: lessons learned from Austrian applications. J. Clean. Prod. 88 (2015), 125-131.

[16] M. Tous, B. Ladislav, L. Houdková, M. Pavlas, P. Stehlík, Waste-to energy (W2E) software- a support tool for decision making process. Brno University of Technology, Institute of Process and Environmental Engineering, Chemical Engineering Transactions volume 18 (2009).

[17] I. Pijákovà, J. Derco, Application of Dynamic Simulations for Assessment of Urban Wastewater Systems Operation. Chem. Biochem. Eng. Q. 29 (2015) 55-62.

[18] P.L. McCarty, J. Bae, J. Kim, Domestic wastewater treatment as a net energy producer–can this be achieved? Environ. Sci. Technol. 45 (2011) 7100–7106.

[19] J.B. Giménez, A. Robles, L. Carretero, F. Durán, M.V. Ruano, M.N. Gattib, J. Ribes, J. Ferrer, A. Seco, Experimental study of the anaerobic urban wastewater treatment in a submerged hollow-fiber membrane bioreactor at semi-industrial scale, Bioresour. Technol. 102 (2011) 8799–8806.

[20] A. L, Smith, L.B. Stadler, L. Cao, N.G, Love, L. Raskin, S.J. Skerlos, Navigating Wastewater Energy Recovery 1 Strategies: A Life Cycle Comparison of Anaerobic Membrane Bioreactor and Conventional Treatment Systems with Anaerobic Digestion, Environ Sci. Technol. 48 (2014), 5972-5981

[21] R. Barat, J. Serralta, M.V. Ruano, E. Jiménez, J. Ribes, A. Seco, J. Ferrer, Biological Nutrient Removal Model Nº 2 (BNRM2): A general model for Wastewater Treatment Plants, Water Sci. Technol. 67 (2013) 1481–1489.

[22] F. Durán, Mathematical modelling of the anaerobic urban wastewater treatment including sulphate-reducing bacteria. Application to an anaerobic membrane bioreactor (Modelación matemática del tratamiento anaerobio de aguas residuales urbanas incluyendo las bacterias sulfatorreductoras, Aplicación a un biorreactor anaerobio de membranas), Ph.D. thesis, Dept. of Hydraulic Engineering and Environment, Universitat Politècnica de València, Spain. 2013.

[23] S.J. Judd, and C. Judd, Principles and Applications of Membrane Bioreactors in Water and Wastewater Treatment. Second Edition, Elsevier, London, UK. 2011.

[24] R. Pretel, A. Robles, M.V. Ruano, A. Seco, J. Ferrer, Environmental impact of submerged anaerobic MBR (AnMBR) technology used to treat urban wastewater at different temperatures. Bioresource Technol. 149 (2013), 532-40.

[25] EPA. Catalog of Biomass Combined Heat and Power Catalog of Technologies, 2007. Available on: http://www.epa.gov/chp/documents/biomass_chp_catalog.pdf (Acceded 5 May 2015)

[26] PSE Probiogas, 2010. Development of sustainable systems of biogas production and use in Spain. Funded by the Ministry of science and innovation. Spanish government, Madrid. Retrieved May 5, 2012,http://213.229.136.11/bases/ainia_probiogas.nsf/0/F9F832A77BF0CA25C125753F0058C4B2/$FILE/Cap2.pdf

[27] J. Serralta, J. Ferrer, L. Borrás, A. Seco, An extension of ASM2d including pH calculation. Water Res. 38 (2004), 4029-4038.

[28] J. Chanona, J. Ribes, A. Seco, J. Ferrer, Optimum design and operation of primary sludge fermentation schemes for volatile fatty acids production. Water Res. 40(2006), 53-60.

[29] M.N. Gatti, Characterization of wastewaters and calibration of the mathematical model BNRM1 for simulation of the biological removal process of organic matter and nutrients (Caracterización de las aguas residuales y calibración del modelo matemático BNRM1 para la simulación de los procesos de eliminación biológica de materia orgánica y nutrientes). Ph.D. thesis, Dept. of Hydraulic Engineering and Environment, Universitat de València, Spain. 2009.

[30] M.V. Ruano, J. Serralta, J. Ribes, F. Garcia-Usach, A. Bouzas, R. Barat, A. Seco, J. Ferrer, Application of the General Model “Biological Nutrient Removal Model No.1” to upgrade two full-scale WWTPs. Environ.Technol. 33 (2011), 1005-1012.

[31] J. Ferrer, R. Pretel, F. Durán, J.B Giménez, A. Robles, M.V. Ruano, J. Serralta, J. Ribes, A. Seco, Design methodology for anaerobic membrane bioreactors (AnMBR): A case study, Sep. Purif. Technol. 141 (2015), 378-386. [32] R. Pretel, A. Robles, M.V. Ruano, A. Seco, J. Ferrer, Filtration process cost in anaerobic membrane bioreactors (AnMBRs) for urban wastewater treatment. Sep. Sci. Technol. In press (2015).

[33] A. Robles, F. Durán, M.V. Ruano, J. Ribes, A. Rosado, A. Seco, J. Ferrer, Instrumentation, control, and automation for submerged anaerobic membrane bioreactors. Environ. Technol. 25 (2015) 1-12.

[34] AEMET, 2015. State Meteorological Agency (Agencia Estatal de Meteorología). Register of hourly and daily average ambient temperature from 2010 to 2014 located in Valencia.

[35] T.E. Daubert, R.P. Danner, H.M. Sibul, C.C. Stebbins, Physical and thermodynamic properties of Pure Compounds: Data compilation, Taylor & Francis, Bristol, PA. 1994.

Table and Figure captions

Table 1. Equations used for determining power energy requirements in WWTPs.

Table 2. Equations used for determining heat energy requirements in WWTPs.

Table 3. Molar enthalpy at the operating temperature of the biological reactions in wastewater treatment system. $\mathbf{X_{OHO}}$: heterotrophic organisms; $\mathbf{X_{PAO}}$: polyphosphate accumulating organism; $\mathbf{X_{PAO,\,PP}}$: poly-phosphate stored by X_{PAO}; $\mathbf{X_{PAO,\,stor}}$: poly-hydroxy-alkanoates stored by X_{PAO}; $\mathbf{X_{AOO}}$: ammonium oxidizing organisms; $\mathbf{X_{NOO}}$: nitrite oxidizing organisms; $\mathbf{X_{AO}}$: acidogenic bacteria; $\mathbf{X_{PRO}}$: acetogenic bacteria; $\mathbf{X_{ACO}}$: methanogenic acetoclastic organisms; $\mathbf{X_{HMO}}$: methanogenic hydrogenotrophic organisms; $\mathbf{S_F}$: sucrose; $\mathbf{S_{Ac}}$: acetate; $\mathbf{S_{VFA}}$: propionate; $\mathbf{S_{NO3}}$: nitrate; and $\mathbf{S_{NO2}}$: total nitrite concentration.

Table 4. Equations used for determining the energy recovery from methane and hydrogen capture in WWTPs.

Table 5. Characteristics of the wastewater entering the designed WWTPs (**sulphate-rich municipal wastewater; **low-sulphate municipal wastewater*).

Figure 1. Flow diagram related to temperature and heat energy requirements in a closed-air treatment unit.

Figure 2. Main window of DESASS including the layout of the **(a)** CAS- and **(b)** AnMBR-based WWTPs (coupled to AeMBR-based post-treatment) evaluated in this study.

Figure 3. Weighted average distribution of the energy input and output in CAS and AnMBR (coupled to an AeMBR- or CAS-based post-treatment and treating 100 and 10 mg SO_4-$S \cdot L^{-1}$) for UWW treatment.

Figure 4. Experimental and simulated temperature considering null heat energy requirements in the AnMBR plant during a: **(a)** 24-hour operating period; **(b)** 24-hour operating period; and **(c)** 30-day operating period.

Figure 5. Simulated heat energy requirements ($kcal \cdot m^{-3}$) at controlled temperature of 20ºC in the AnMBR plant during a: **(a)** 24-hour operating period (heating requirements); **(b)** 24-hour operating period (cooling requirements); and **(c)** 30-day operating period.

Table 1. Equations used for determining power energy requirements in WWTPs.

Power Energy	Equation	
Power energy consumed by the blower, P_B in $J \cdot s^{-1}$	$\frac{(M \cdot R \cdot T_{gas})}{(\alpha-1)\cdot\eta_{blower}}\left[\left(\frac{p_2}{p_1}\right)^{\frac{\alpha-1}{\alpha}}-1\right]$	Eq.2
Absolute outlet pressure, P_2 in atm	$\left\{p_1\cdot 10^5+\Delta h_{difussers}+Y_{reactor}\cdot\rho_{liquor}\cdot g+\left[\left(\frac{2\cdot(L+Leq)f\cdot V^2\cdot\rho}{D}\right)\text{inlet.}+\left(\frac{2\cdot(L+Leq)f\cdot V^2\cdot\rho}{D}\right)\text{outlet.}\right]\right\}x10^{-5}$	Eq.3
Power energy consumed by the general pump, P_g in $J \cdot s^{-1}$	$q_{imp}\cdot\rho\cdot g\cdot\frac{\left\{\left[\left(\frac{(L+Leq)\cdot f\cdot V^2}{D\cdot 2\cdot g}\right)\text{inlet}+\left(\frac{(L+Leq)f\cdot V^2}{D\cdot 2\cdot g}\right)\text{outlet}\right]+[Z_1-Z_2]\right\}}{\eta_{pump}}$	Eq.4
Power energy consumed during filtration, degasification or back-flushing, P_{stage} in $J \cdot s^{-1}$	$\frac{q_{stage}\cdot TMP_{stage}}{\eta_{pump}}$	Eq.5
Power energy consumed by the stirrer, $P_{stirrer}$ in $J \cdot s^{-1}$	$\frac{E_{stirrer}\cdot V_{reactor}}{\eta_{engine}}$	Eq.6
Power energy consumed by the sludge dewatering system, $P_{dewatering}$ in $kWh \cdot d^{-1}$	$\frac{E_{dewatering}\cdot M_{MLSS}}{\eta_{engine}}$	Eq.7

Symbols

M	Molar flow rate of gas, $mol \cdot s^{-1}$
R	Gas constant for gas, $J \cdot mol^{-1} \cdot K^{-1}$
P_1	Absolute inlet pressure, atm
P_2	Absolute outlet pressure, atm
T_{gas}	Gas temperature, K
α	Adiabatic index
η_{blower}	Blower efficiency
$Ah_{difussers}$	Diffusers pressure drops, Pa
$Y_{reactor}$	Sludge level in the reactor, m
ρ	Sludge density, $kg \cdot m^{-3}$
g	Acceleration of gravity, $m \cdot s^{-2}$
$\frac{2\cdot(L+L_{eq})\cdot f\cdot V^2\cdot\rho}{D}$	Linear and accidental pressure drops, Pa
$q_{imp.}$	Impulsion volumetric flow rate, $m^3 \cdot s^{-1}$
L	Pipe length, m
L_{eq}	Equivalent pipe length of accidental pressure drops, m
V	Velocity, $m \cdot s^{-1}$
f	Friction factor
d	Diameter, m,
Z_1-Z_2	Height difference, m
η_{pump}	Pump efficiency
TMP_{stage}	Transmembrane pressure, Pa
q_{stage}	Pump volumetric flow rate, $m^3 \cdot s^{-1}$
$E_{Stirrer}$	Specific power energy of the stirrer, $w \cdot m^{-3}$
η_{engine}	Engine efficiency
$E_{dewatering}$	Specific energy consumption of the dewatering system, $kWh \cdot tSS^{-1}$
M_{MLSS}	Mass flow, $tSS \cdot d^{-1}$

Table 2. Equations used for determining heat energy requirements in WWTPs.

Heat Energy	Equation	
External heat energy required, $Q_{EXTERNAL}$ in kcal·h^{-1}	$C_P water \cdot q \cdot \rho \cdot \left(T_{fixed} - T_{\inf low} \right)$	Eq.8
Heat energy dissipated through walls, $Q_{DISSIPATED}$ in kcal·h^{-1}	$\Sigma U \cdot S \cdot \Delta T$	Eq.9
Heat transfer coefficient in the non-buried section of the reactor, $U_{non\text{-}baried}$ in kcal·h^{-1}·m^{-2}·k^{-1}	$\frac{1}{\Sigma \frac{\delta_{reactor}}{K_{reactor}} + \frac{1}{h_{air}}}$	Eq.10
Heat transfer coefficient in the buried section of the reactor, U_{buried} in kcal·h^{-1}·m^{-2}·k^{-1}	$\frac{1}{\Sigma \frac{\delta_{reactor}}{K_{reactor}} + \frac{\delta_{soil}}{K_{soil}}}$	Eq.11
Soil conductivity, *Ks* in kcal· m^{-1}·h^{-1}·°C^{-1}	0.025 · % humidity + 1.2	Eq.12
Heat energy released/absorbed after gas decompression, $Q_{DESCOMPRESSION}$ in kcal·h^{-1}	$\frac{R \cdot T}{\alpha - 1}\left[\left(\frac{P_1}{P_2} \right)^{\frac{\alpha-1}{\alpha}} - 1 \right] \cdot \frac{M}{\Sigma (MW \cdot \%)_i \cdot 4.187}$	Eq.13
Gas temperature (considering heat dissipated through the pipe), $T_{GAS,PIPES}$ in K	$\frac{\Sigma (Cp_i \cdot (T) \cdot \%_i) \{ \frac{M}{\Sigma (MW \cdot \%)_i \cdot 4.187} \} \cdot T - \Sigma \frac{K_{pipe}}{\delta_{pipe}} \cdot S_{pipe} \cdot (\Delta T)}{\Sigma (Cp_i \cdot (T) \cdot \%_i) \{ \frac{M}{\Sigma (MW \cdot \%)_i \cdot 4.187} \}}$	Eq.14
Gas temperature increase during compression, $T_{GAS,COMPRESSION}$ in K	$(\frac{P_2}{P_1})^{\alpha - 1/\alpha} \cdot T$	Eq.15
Molar enthalpy of the reaction at a given temperature, ΔH_T in kcal·mol^{-1}	$\left(\eta \Delta H^{\circ}_F \right)_{PRODUCTS} - \left(\eta \Delta H^{\circ}_F \right)_{REACTANTS} + \int_{298.15}^{T} \Sigma \eta \cdot C_P$	Eq.16
Specific heat for solids and liquids, $Cp_{solids\text{-}liquids}$ in kcal·kmol^{-1}·K^{-1}	$\left(A + BT + CT^2 + DT^3 + ET^4 \right) \cdot 2.39 \cdot 10^{-7}$	Eq.17
Specific heat for gases, Cp_{gases} in kcal·kmol^{-1}·K^{-1}	$\left(A + B \left[\left(\frac{\frac{C}{T}}{\sinh\left(\frac{C}{T} \right)} \right) \right]^2 + D \left[\left(\frac{\frac{E}{T}}{\sinh\left(\frac{E}{T} \right)} \right) \right]^2 \right) \cdot 2.39 \cdot 10^{-7}$	Eq.18
Specific heat for dissolved methane, $Cp_{methane}$ in kcal·kmol^{-1}·K^{-1}	$\left(\frac{A^2}{1 - \frac{T}{Tc}} + B - 2AC\,(1 - \frac{T}{Tc}) - AD\,(1 - \frac{T}{Tc})^2 - \frac{C^2\,(1 - \frac{T}{Tc})^3}{3} - \frac{CD\,(1 - \frac{T}{Tc})^4}{2} - \frac{D^2\,(1 - \frac{T}{Tc})^5}{5} \right) \cdot 2.39 \cdot 10^{-7}$	Eq.19
Heat released/absorbed by biological reactions in the treatment unit, $Q_{ENTHALPY}$ in kcal·h^{-1}	$\Sigma (\frac{r_x \cdot v_{x,y}}{MW} x \Delta H_T)_i \, Vx \frac{1}{24}$	Eq.20

Symbols

C_{Pwater}	Specific heat, 1 Kcal·Kg^{-1}·K^{-1} for water
q	Inlet flow rate, m^3·h^{-1}
ρ	Sludge density, kg·m^{-3}
T_{fixed}-T_{inflow}	Difference between the intake temperature and the temperature set-point, K
U	Overall heat transfer coefficient, Kcal·h^{-1}·m^{-2}·K^{-1}
$S_{reactor}$	Surface of the reactor/pipe, m^2

ΔT	Difference in temperature between the inside and the outside of the reactor/pipe, K
$\delta_{reactor}$	Reactor thickness, m
δ_{soil}	Thickness of the soil in contact with the reactor wall, m
$k_{reactor}$	Conductivity of the reactor material, $Kcal \cdot h^{-1} \cdot m^{-1} \cdot K^{-1}$
h_{air}	Convective heat transfer coefficient of the air, 12 $Kcal \cdot h^{-1} \cdot m^{-2} \cdot K^{-1}$
k_{soil}	Soil conductivity, $Kcal \cdot h^{-1} \cdot m^{-1} \cdot K^{-1}$
M	Mass flow rate of gas, $Kg \cdot h^{-1}$
T	Compound temperature, K
K_{pipe}	Conductivity of the pipe material, $Kcal \cdot h^{-1} \cdot m^{-1} \cdot K^{-1}$
δ_{pipe}	Pipe thickness, m
MW	Molecular weight, $g \cdot mol^{-1}$
P_1	Absolute inlet pressure, atm
P_2	Absolute outlet pressure, atm
α	Adiabatic index
$\Delta H^o_{F,\ PRODUCTS}$	Enthalpy of the products at 298.15 K, $Kcal \cdot mol^{-1}$
$\Delta H^o_{F,\ REACTANTS}$	Enthalpy of the reactants at 298.15 K, $Kcal \cdot mol^{-1}$
η	Stoichiometric number
C_P	Specific heat of each component of the reaction, $Kcal \cdot mol^{-1} \cdot K^{-1}$
A, B, C, D, E	Specifics constants for the compounds (listed in Table 1)
Tc	Critic temperature of the dissolved methane, 190.3K
$R_x \cdot \nu_{x,y}$	Speed of the generation/degradation of the main compound of the reaction, $mg \cdot l^{-1} \cdot d^{-1}$
ΔH_T	Enthalpy of the reaction at a given temperature, $Kcal \cdot mol^{-1}$
V	Volume of the biological reaction, m^3

Table 3. Molar enthalpy at the operating temperature of the biological reactions in wastewater treatment system. $\mathbf{X_{OHO}}$: heterotrophic organisms; $\mathbf{X_{PAO}}$: polyphosphate accumulating organism; $\mathbf{X_{PAO,\,PP}}$: poly-phosphate stored by X_{PAO}; $\mathbf{X_{PAO,\,stor}}$: poly-hydroxy-alkanoates stored by X_{PAO}; $\mathbf{X_{AOO}}$: ammonium oxidizing organisms; $\mathbf{X_{NOO}}$: nitrite oxidizing organisms; $\mathbf{X_{AO}}$: acidogenic bacteria; $\mathbf{X_{PRO}}$: acetogenic bacteria; $\mathbf{X_{ACO}}$: methanogenic acetoclastic organisms; $\mathbf{X_{HMO}}$: methanogenic hydrogenotrophic organisms; $\mathbf{S_F}$: sucrose; $\mathbf{S_{Ac}}$: acetate; $\mathbf{S_{VFA}}$: propionate; $\mathbf{S_{NO3}}$: nitrate; and $\mathbf{S_{NO2}}$: total nitrite concentration.

Aerobic growth of X_{OHO} over S_F	$C_{12}H_{22}O_{11}+ 12O_2 \rightarrow 12CO_2+11H_20$	$\Delta H^o_{T,1=} (12\cdot\Delta H^o_{CO2}+11\cdot\Delta H^o_{H2O}) - (\Delta H^o_{C12H22O11}) + \int_{298.15}^{T}[12\cdot CpCO2 + 11\cdot CpH2O - CpC12H22O11 - 12\cdot CpO2]\cdot(T-298.15)$
Aerobic growth of X_{OHO} over S_{Ac}	$CH_3COOH+ 2O_2 \rightarrow 2CO_2+2H_20$	$\Delta H^o_{T,2=} (2\cdot\Delta H^o_{CO2}+2\cdot\Delta H^o_{H2O}) - (\Delta H^o_{CH3COOH} + \int_{298.15}^{T}[2\cdot CpCO2 + 2\cdot CpH2O - CpCH3COOH - 2\cdot CpO2]\cdot(T-298.15)$
Aerobic growth of X_{OHO} over S_{VFA}	$CH_3CH_2COOH+ \frac{7}{2}O_2 \rightarrow 3CO_2+3H_20$	$\Delta H^o_{T,3=} (3\cdot\Delta H^o_{CO2}+3\cdot\Delta H^o_{H2O}) - (\Delta H^o_{CH3CH2COOH}) + \int_{298.15}^{T}[3\cdot CpCO2 + 3\cdot CpH2O) - CpCH3CH2COOH - \frac{7}{2}\cdot CpO2]\cdot(T-298.15)$
Anoxic growth of X_{OHO} over S_F and S_{NO3}	$C_{12}H_{22}O_{11}+ 8NO_3 \rightarrow 12CO_2+11H_20+4N_2$	$\Delta H^o_{T,4=} (12\cdot\Delta H^o_{CO2}+11\cdot\Delta H^o_{H2O}) - (\Delta H^o_{C12H22O11}+ 8\cdot\Delta H^o_{NO3}) + \int_{298.15}^{T}[12\cdot CpCO2 + 11\cdot CpH2O + 4\cdot CpN2 - CpC12H22O11 - 8\cdot CpNO3]\cdot(T-298.15)$
Anoxic growth of X_{OHO} over S_{Ac} and S_{NO3}	$CH_3COOH + \frac{4}{3}NO_3 \rightarrow 2CO_2+2H_20+\frac{4}{6}N_2$	$\Delta H^o_{T,5=} (2\cdot\Delta H^o_{CO2}+2\cdot\Delta H^o_{H2O}) - (\Delta H^o_{CH3COOH} + \frac{4}{3}\cdot\Delta H^o_{NO2}) + \int_{298.15}^{T}[2\cdot CpCO2 + 2\cdot CpH2O + \frac{4}{6}\cdot CpN2 - CpCH3COOH - \frac{4}{3}\cdot CpNO2]\cdot(T-298.15)$
Anoxic growth of X_{OHO} over S_{VFA} and S_{NO3}	$CH_3CH_2COOH+\frac{7}{3}NO_3 \rightarrow 6CO_2+6H_20+2N_2$	$\Delta H^o_{T,6=} (6\cdot\Delta H^o_{CO2}+6\cdot\Delta H^o_{H2O} - (\frac{7}{3}\cdot\Delta H^o_{NO3}+ \Delta H^o_{CH3CH2COOH}) + \int_{298.15}^{T}[6\cdot CpCO2 + 6\cdot CpH2O + 2\cdot CpN2 - CpCH3CH2COOH - \frac{7}{3}\cdot CpNO3]\cdot(T-298.15)$
Anoxic growth of X_{OHO} over S_F and S_{NO2}	$C_{12}H_{22}O_{11}+ 12NO_2 \rightarrow 12CO_2+11H_20+6N_2$	$\Delta H^o_{T,7=} (12\cdot\Delta H^o_{CO2}+11\cdot\Delta H^o_{H2O}) - (\Delta H^o_{C12H22O11}+ 12\cdot\Delta H^o_{NO2}) + \int_{298.15}^{T}[12\cdot CpCO2 + 11\cdot CpH2O + 6\cdot CpN2 - CpC12H22O11 - 12\cdot CpNO2]\cdot(T-298.15)$
Anoxic growth of X_{OHO} over S_{Ac} and S_{NO2}	$CH_3COOH + 2NO_2 \rightarrow 2CO_2+2H_20+2N_2$	$\Delta H^o_{T,8=} (2\cdot\Delta H^o_{CO2}+2\cdot\Delta H^o_{H2O}) - (\Delta H^o_{CH3COOH} + 2\cdot\Delta H^o_{NO2}) + \int_{298.15}^{T}[2\cdot CpCO2 + 2\cdot CpH2O + 2\cdot CpN2 - CpCH3COOH - 2\cdot CpNO2]\cdot(T-298.15)$
Anoxic growth of X_{OHO} over S_{VFA} and S_{NO2}	$CH_3CH_2COOH+\frac{7}{2}NO_2 \rightarrow 3CO_2+3H_20+\frac{7}{4}N2$	$\Delta H^o_{T,9=} (3\cdot\Delta H^o_{CO2}+3\cdot\Delta H^o_{H2O}) - (\Delta H^o_{CH3CH2COOH} + \frac{7}{2}\cdot\Delta H^o_{NO2}) + \int_{298.15}^{T}[3\cdot CpCO2 + 3\cdot CpH2O + \frac{7}{4}\cdot CpN2 - CpCH3CH2COOH - \frac{7}{2}\cdot CpNO2]\cdot(T-298.15)$
Storage of $X_{PAO,\,Stor}$ over S_{Ac}	$(CH_3COOH)1/2 + 0.5(C_6H_{10}O_5)1/6 + 0.44HPO_3 \rightarrow 1.33(C_4H_6O_2)1/4 + 0.44H_3PO_4 + 0.17CO_2 + 0.023H_2O$	$\Delta H^o_{T,10=} = (1.33\cdot\Delta H^o_{PHA}+0.17\cdot\Delta H^o_{CO2}+0.44\cdot\Delta H^o_{phosphoric}+0.023\cdot\Delta H^o_{H2O}) - (\Delta H^o_{CH3COOH} + 0.5\cdot\Delta H^o_{glycogen} +0.44\cdot\Delta H^o_{PP}) + \int_{298.15}^{T}[1.33\cdot CpPHA + 0.17\cdot CpCO2 + 0.44\cdot Cpphosphoric + 0.023\cdot CpH2O - CpCH3COOH - 0.5\cdot Cpglycogen - 0.44\cdot CpPP]\cdot(T-298.15)$
Storage of $X_{PAO,\,Stor}$ over S_{VFA}	$(CH_3CH_2COOH)1/3 +0.5(C_6H_{10}O_5)1/6 + 0.44HPO_3 \rightarrow 1.23(C_4H_6O_2) 1/4 + 0.44H_3PO_4 +0.27CO_2 + 0.023H_2O$	$\Delta H^o_{T,11=} (1.23\cdot\Delta H^o_{PHA}+0.27\cdot\Delta H^o_{CO2}+0.44\cdot\Delta H^o_{phosphoric}+0.023\cdot\Delta H^o_{H2O}) - (\Delta H^o_{CH3CH2COOH} + 0.5\cdot\Delta H^o_{glycogen}+0.44\cdot\Delta H^o_{PP}) + \int_{298.15}^{T}[1.23\cdot CpPHA + 0.27\cdot CpCO2 + 0.44\cdot Cpphosphoric + 0.023\cdot CpH2O - CpCH3CH2COOH - 0.5\cdot Cpglycogen - 0.44\cdot CpPP]\cdot(T-298.15)$

Aerobic storage of $X_{PAO,\ PP}$	$C_4H_6O_2$+ $H3PO_4$ +$\frac{9}{2}O_2$ → HPO_3 + $4CO_2$+$4H_2O$	$\Delta H^o_{T,12=}$ ($4\cdot\Delta H^o_{CO2}$+$4\cdot\Delta H^o_{H2O}$+ΔH^o_{PP})- (ΔH_{PHA}+ ΔH_{H3PO4}) + $\int_{298.15}^{T}[4\cdot CpCO2 + 4\cdot CpH2O + CpPP - CpPHA - CpH3PO4 - \frac{9}{2}\cdot CpO2]\cdot(T-298.15)$
Anoxic storage of $X_{PAO,\ PP}$ over S_{NO3}	$C_4H_6O_2$+ H_3PO_4+$\frac{9}{3}NO_3$ → HPO_3 + $4CO_2$+$4H_2O$+$\frac{9}{6}N_2$	$\Delta H^o_{T,13=}$ ($4\cdot\Delta H^o_{CO2}$+$4\cdot\Delta H^o_{H2O}$+ΔH^o_{PP})- (ΔH^o_{PHA}+ ΔH^o_{H3PO4} +$\frac{9}{3}\cdot\Delta H^o_{NO3}$) +$\int_{298.15}^{T}[4\cdot CpCO2 + 4\cdot CpH2O + CpPP + \frac{9}{6}\cdot CpN2 - CpPHA - CpH3PO4 - \frac{9}{3}\cdot CpNO3]\cdot(T-298.15)$
Anoxic storage of $X_{PAO,\ PP}$ over S_{NO2}	$C_4H_6O_2$+ H_3PO_4 +$\frac{9}{2}NO_2$ → HPO_3+ $4CO_2$+$4H_2O$ +$\frac{9}{4}N_2$	$\Delta H^o_{T,14=}$($4\cdot\Delta H^o_{CO2}$+$4\cdot\Delta H^o_{H2O}$+ΔH^o_{PP})- (ΔH^o_{PHA}+ ΔH^o_{H3PO4} +$\frac{9}{2}\cdot\Delta H^o_{NO2}$) +$\int_{298.15}^{T}[4\cdot CpCO2 + 4\cdot CpH2O + CpPP - p + \frac{9}{4}\cdot CpN2 - CpPHA - CpH3PO4 - \frac{9}{2}\cdot CpNO2]\cdot(T-298.15$
Aerobic growth on X_{PAO}	$C_4H_6O_2$ + $\frac{9}{2}O_2$ → $4CO_2$+$3H_2O$	$\Delta H^o_{T,15=}$ ($4\cdot\Delta H^o_{CO2}$+$3\cdot\Delta H^o_{H2O}$)- (ΔH^o_{PHA}) +$\int_{298.15}^{T}[4\cdot CpCO2 + 3\cdot CpH2O - CpPHA - \frac{9}{2}\cdot CpO2]\cdot(T-298.15)$
Anoxic growth on X_{PAO} over S_{NO3}	$C_4H_6O_2$ + $\frac{9}{3}NO_3$ → $\frac{9}{6}N_2$+$4CO_2$+$3H_2O$	$\Delta H^o_{T,16=}$ ($4\cdot\Delta H^o_{CO2}$+$3\cdot\Delta H^o_{H2O}$)- (ΔH^o_{PHA}+ $\frac{9}{3}\cdot\Delta H^o_{NO2}$) + $\int_{298.15}^{T}[4\cdot CpCO2 + 3\cdot CpH2O + \frac{9}{6}\cdot CpN2 - CpPHA - \frac{9}{3}\cdot CpNO2]\cdot(T-298.15)$
Anoxic growth on X_{PAO} over S_{NO2}	$C_4H_6O_2$ + $\frac{9}{2}NO_2$ → $\frac{9}{4}N_2$+$4CO_2$+$3H_2O$	$\Delta H^o_{T,17=}$ ($4\cdot\Delta H^o_{CO2}$+$4\cdot\Delta H^o_{H2O}$)- (ΔH^o_{PHA}+ $\frac{9}{2}\cdot\Delta H^o_{NO2}$) + $\int_{298.15}^{T}[4\cdot CpCO2 + 4\cdot CpH2O + \frac{9}{4}\cdot CpN2 - CpPHA - \frac{9}{2}\cdot CpNO2]\cdot(T-298.15)$
Total nitrification	NH_4^+ +2 O_2 → NO_3^- +$2H^+$+ H_20	$\Delta H^o_{T,18=}$ (ΔH^o_{H2O}+ΔH^o_{NO3})- (ΔH^o_{NH4}) +$\int_{298.15}^{T}[CpH2O + CpNO3 - CpNH4 - 2\cdot CpO2]\cdot(T-298.15)$
Ammonium anaerobic oxidation (Sharon-Anammox process)	$NH4^+ + NO2^-$ → N2 + 2H20	$\Delta H^o_{T,18=}$ ($2\cdot\Delta H^o_{H2O}$-(ΔH^o_{NO2}+ΔH^o_{NH4}) + $\int_{298.15}^{T}[2\cdot CpH2O + CpN2 - CpNH4 - CpNO2]\cdot(T-298.15)$
Aerobic growth of X_{AOO}	NH_4^+ +$\frac{3}{2}O_2$ → NO_2^- +$2H^+$+ H_20	$\Delta H^o_{T,19=}$ (ΔH^o_{H2O}+ΔH^o_{NO2})- (ΔH^o_{NH4}) +$\int_{298.15}^{T}[CpH2O + CpNO2 - CpNH4 - \frac{3}{2}\cdot CpO2]\cdot(T-298.15)$
Aerobic growth of X_{NOO}	NO_2^- +$\frac{1}{2}O_2$ → NO_3^-	$\Delta H^o_{T,20=}$ (ΔH^o_{NO3})- (ΔH^o_{NO2}) + $\int_{298.15}^{T}[CpNO3 - CpNO2 - \frac{1}{2}\cdot CpO2]\cdot(T-298.15)$
Anaerobic growth of X_{AO} (Acidogenesis)	$C_{12}H_{22}O_{11}$+$3H_2O$ → $2CH_3COO^-$ + $2CH_3CH_2COO^-$ +$2HCO_3^-$ + $6H^+$ + $2H_2$	$\Delta H^o_{T,21=}$($2\cdot\Delta H^o_{CH3COOH}$ + $2\cdot\Delta H^o_{CH3CH2COOH}$ +$2\cdot\Delta H^o_{HCO3}$)- ($\Delta H^o_{C12H22O11}$ +$3\cdot\Delta H^o_{H2O}$) +$\int_{298.15}^{T}[2\cdot CpH2 + 2\cdot CpCH3COOH + 2\cdot CpCH3CH2COOH + 2\cdot CpHCO3 - 3\cdot CpH2O - CpC12H22O11]\cdot(T-298.15)$
Anaerobic growth of X_{PRO} (Acetogenesis)	$CH_3CH_2COO^-$+$3H_2O$ → CH_3COO^- + HCO_3^- + H^+ + $3H_2$	$\Delta H^o_{T,22=}$ ($\Delta H^o_{CH3COOH}$ +ΔH^o_{HCO3})- ($\Delta H^o_{CH3CH2COOH}$ +$3\cdot\Delta H^o_{H2O}$) + $\int_{298.15}^{T}[CpCH3COOH + CpHCO3 + 3\cdot CpH2 - CpCH3CH2COOH - 3\cdot CpH2O]\cdot(T-298.15)$
Anaerobic growth of X_{ACO} (Acetoclastic methanogenesis)	CH_3-COO^-+H_2O → CH_4+HCO_3^-	$\Delta H^o_{T,23=}$ (ΔH^o_{CH4}+ΔH^o_{HCO3})- ($\Delta H^o_{CH3COOH}$ +ΔH^o_{H2O}) + $\int_{298.15}^{T}[CpCH4 + CpHCO3 - CpCH3COOH - CpH2O]\cdot(T-298.15)$
Anaerobic growth of X_{HMO} (Hydrogenotrophic methanogenesis)	CO_2+$4H_2$ → CH_4+$2H_2O$	$\Delta H^o_{T,24=}$ (ΔH^o_{CH4}+$2\cdot\Delta H^o_{H2O}$)- (ΔH^o_{CO2}) + $\int_{298.15}^{T}[CpCH4 + 2\cdot CpH2O - CpCO2 - 4\cdot CpH2]\cdot(T-298.15)$
Sulphate reduction to sulphide from acetic acid	CH_3COO^- + SO_4^{2-} → HS^- + $2HCO_3^-$	$\Delta H^o_{T,25=}$ (ΔH^o_{HS}+$2\cdot\Delta H^o_{carbonic}$)- ($\Delta H^o_{CH3COOH}$ +ΔH^o_{SO4}) + $\int_{298.15}^{T}[CpHS + 2\cdot Cpcarbonic - CpCH3COOH - CpSO4]\cdot(T-298.15)$
Sulphate reduction to sulphide from propionic acid	$CH_3CH_2COO^-$+ 0.75 SO_4^{2-} → CH_3COO^- + 0.75 S^{2-} + CO_2	$\Delta H^o_{T,26=}$ ($\Delta H^o_{CH3COOH}$ + $0.75\cdot\Delta H^o_{HS}$+ΔH^o_{CO2})- ($0.75\cdot\Delta H^o_{SO4}$+ $\Delta H^o_{CH3CH2COOH}$) +$\int_{298.15}^{T}[CpCH3COOH + 0.75\cdot CpHS + CpCO2 - 0.75\cdot CpSO4 - CpCH3CH2COOH]\cdot(T-298.15)$
Sulphate reduction to sulphide from H_2	H_2+0.25 SO_4^{2-} + 0.25 H^+ → 0.25 HS^- + H_2O	$\Delta H^o_{T,27=}$ ($0.25\cdot\Delta H^o_{HS}$+ΔH^o_{H2O})- ($0.25\Delta H^o_{SO4}$) +$\int_{298.15}^{T}[0.25\cdot CpHS + CpH2O - 0.25\cdot CpSO4 - CpH2]\cdot(T-298.15)$

Table 4. Equations used for determining the energy recovery from methane and hydrogen capture in WWTPs.

Energy recovery from methane and hydrogen capture in terms of heat, $Q_{methane}$ in kcal·h^{-1}	$\frac{V_{biogas}\cdot\left(\%CH_4\cdot CV_{CH_4}+\%H_2\cdot CV_{H_2}\right)\%_{heat\ effciency\ \ CHP}}{1000\cdot 24\cdot 4.187}\cdot\%_{Heat\ \ exchanger}$	Eq.21
Energy recovery from methane and hydrogen capture in terms of power, $W_{methane}$ in kW	$\frac{V_{biogas}\cdot\left(\%CH_4\cdot CV_{CH_4}+\%H_2\cdot CV_{H_2}\right)\%_{power\ effciency\ \ CHP}}{1000\cdot 24\cdot 3600}$	Eq.22
Allowable value of H_2S in $mg_{H20}\cdot Mj^{-1}{}_{biogas}$	$\frac{\%_{H_2S}\cdot MW_{H_2S}}{\left(\%_{CH_4}\cdot CV_{CH_4}+\%H_2\cdot CV_{H_2}\cdot 22.4\right)\cdot 10^{-3}}$	Eq.23

Symbols

V_{biogas}	Biogas volume, l·d^{-1}
$\%CH_4$	Methane richness, %
CV_{CH4}	Methane calorific power, KJ·m^{-3}
$\%H_2$	Hydrogen richness, %
CV_{H2}	Hydrogen calorific power, KJ·m^{-3}
$\%_{\text{heat efficiency CHP}}$	Heat efficiency of the CHP system, %
$\%_{\text{heat exchanger}}$	Heat exchanger efficiency, %
$\%_{\text{power efficiency CHP}}$	Power efficiency of the CHP system, %
$\%H_2S$	Hydrogen sulphide percentage, %
MW_{H2S}	Hydrogen sulphide molecular weight, mg·m^{-3}

Table 5. Characteristics of the wastewater entering the designed WWTPs (**sulphate-rich municipal wastewater; **low-sulphate municipal wastewater*).

Parameter	**Unit**	**Value**
T-COD	mg COD ·L^{-1}	945
T-BOD	mg COD·L^{-1}	715
S-COD	mg COD ·L^{-1}	285
S-BOD	mg COD·L^{-1}	255
TN	mg N·L^{-1}	47
NH_4-N	mg N·L^{-1}	16
TP	mg P·L^{-1}	13
PO_4-P	mg P·L^{-1}	4
SO_4-S	mg S·L^{-1}	100*/10**
TSS	mg TSS·L^{-1}	429
NVSS	mg NVSS·L^{-1}	100

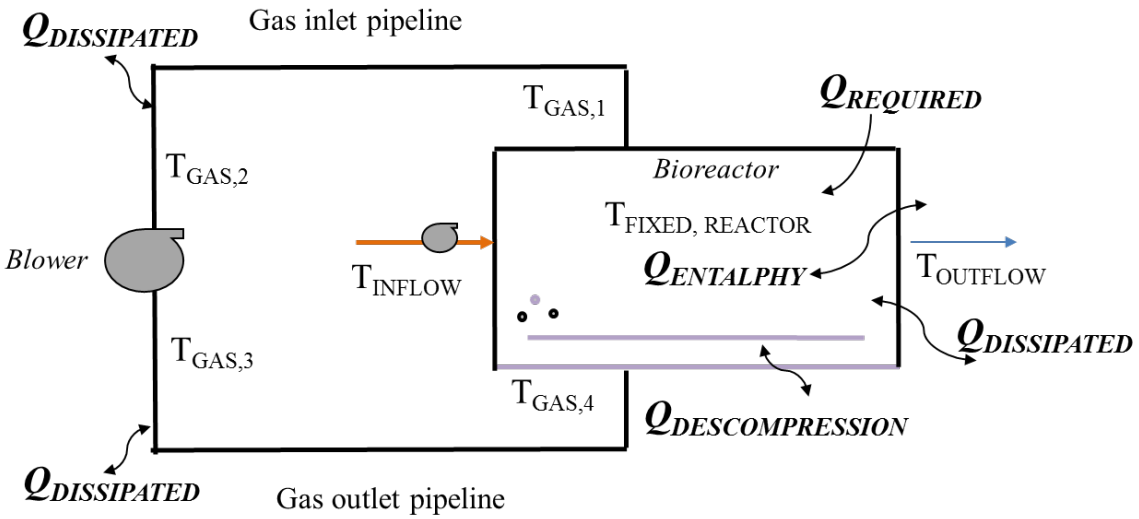

Figure 1. Flow diagram related to temperature and heat energy requirements in a closed-air treatment unit.

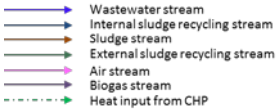

(a)

(b)

Figure 2. Main window of DESASS including the layout of the **(a)** CAS- and **(b)** AnMBR-based WWTPs (coupled to AeMBR-based post-treatment) evaluated in this study. Nomenclature: **ND**: Chamber; **Prim. Settler:** Primary Settler; **Sec. Settler:** Secondary Settler; **Ax Reactor:** Anoxic tank; **Ae Reactor:** Aerobic tank; **Reac.**: Reactant: (FeCl for P removal); **An. Digest.:** Anaerobic Digester; **MBR:** Membrane Bioreactor; **Anaer. R**.: Anaerobic Reactor; **AnMBR**: Anaerobic Membrane Bioreactor.

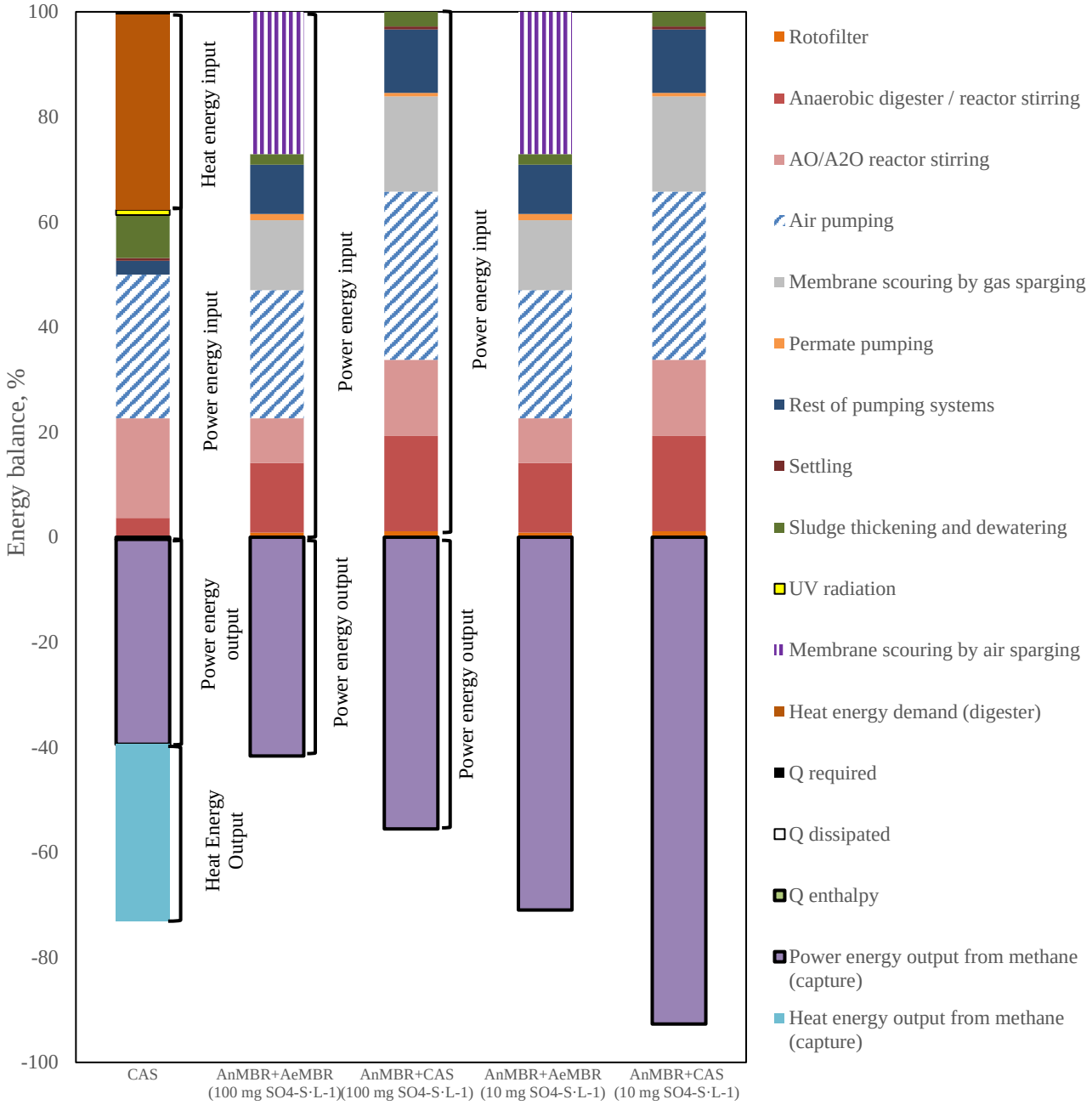

Figure 3. Weighted average distribution of the energy input and output in CAS and AnMBR (coupled to an AeMBR- or CAS-based post-treatment and treating 100 and 10 mg SO_4-S·L^{-1}) for UWW treatment.

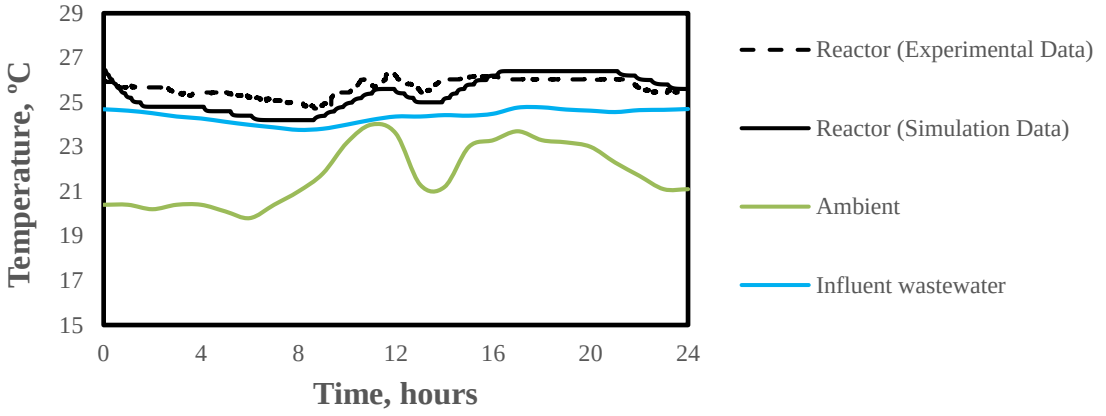

(a)

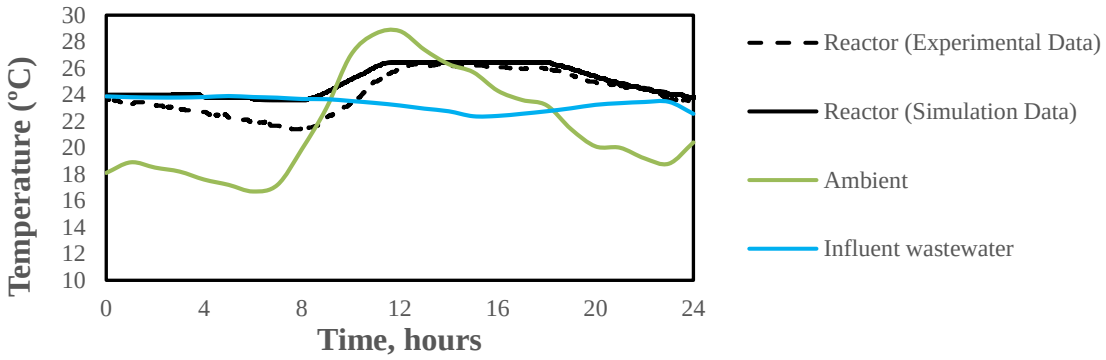

(b)

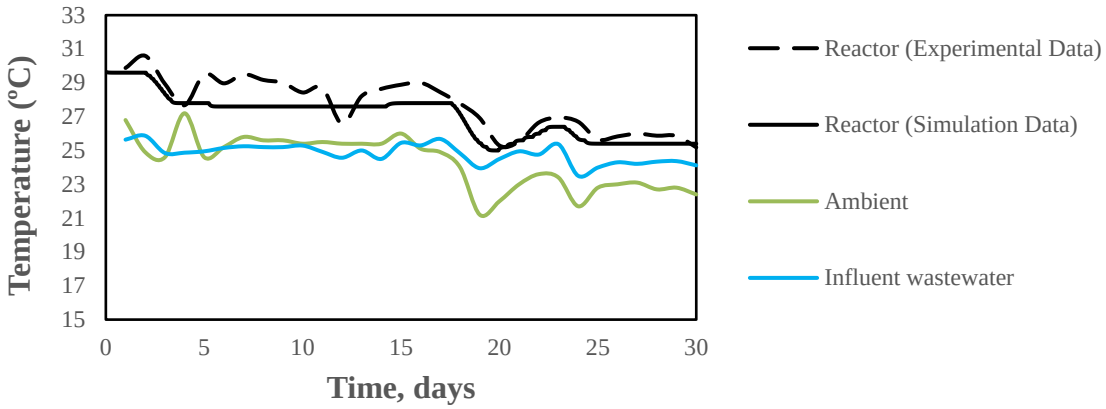

(c)

Figure 4. Experimental and simulated temperature considering null heat energy requirements in the AnMBR plant during a: **(a)** 24-hour operating period; **(b)** 24-hour operating period; and **(c)** 30-day operating period.

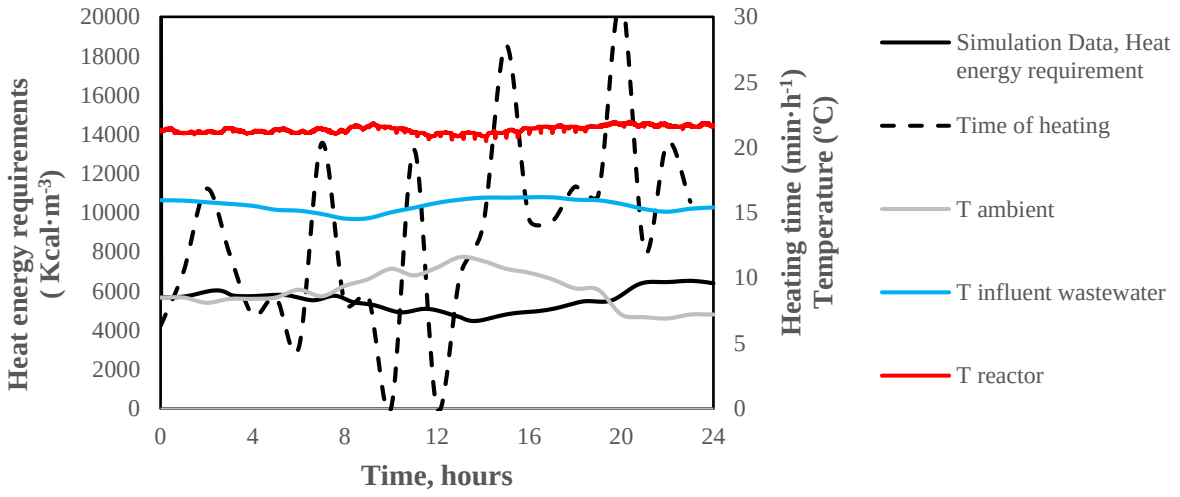

(a)

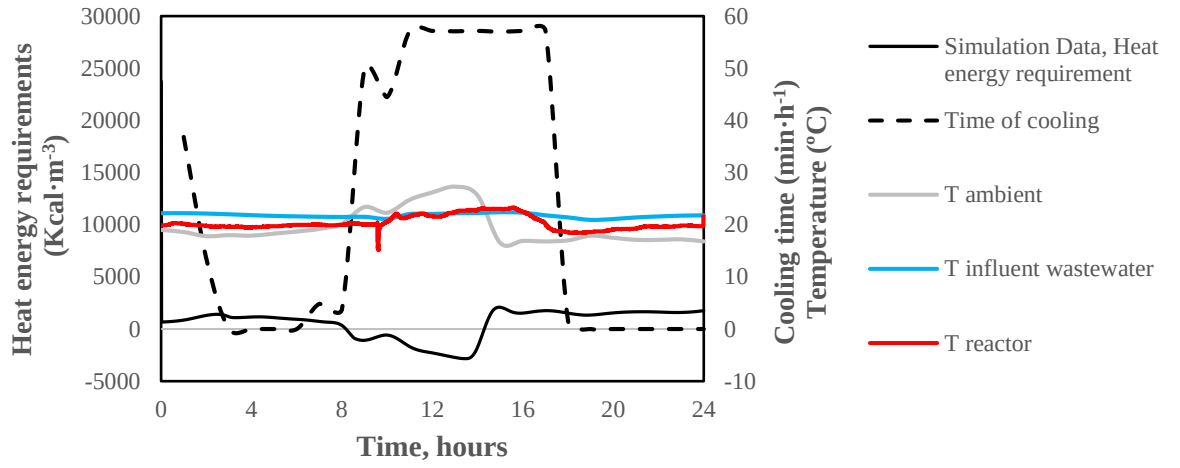

(b)

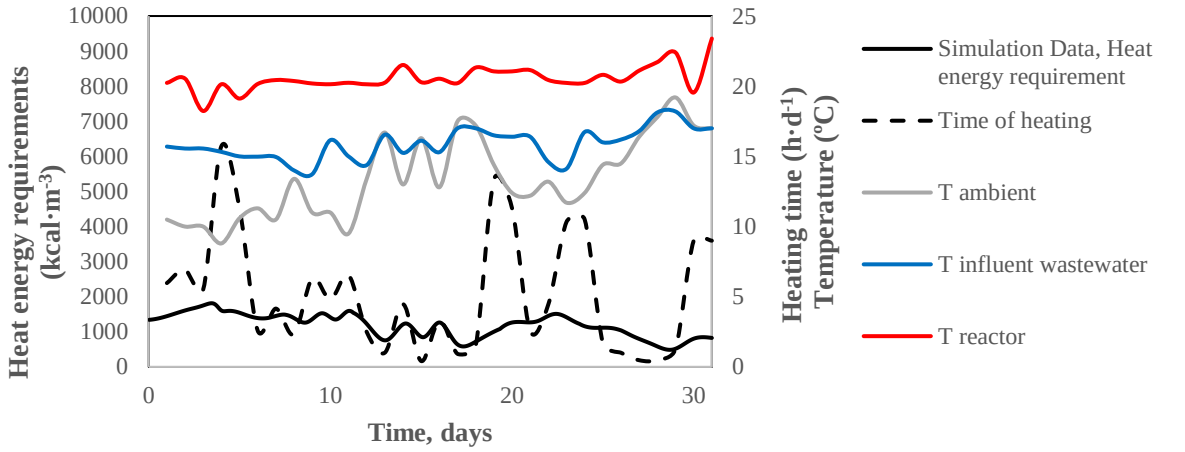

(c)

Figure 5. Simulated heat energy requirements (kcal·m^{-3}) at controlled temperature of 20ºC in the AnMBR plant during a: **(a)** 24-hour operating period (heating requirements); **(b)** 24-hour operating period (cooling requirements); and **(c)** 30-day operating period.